Journal of Solid State Chemistry **156,** 135–142 (2001)
doi:10.1006/jssc.2000.8972, available online at http://www.idealibrary.com on IDEAL®

A New Mixed Framework Compound with Corrugated $[Si_6O_{15}]_{\infty\infty}$ Layers: $K_2TiSi_6O_{15}$[1]

Xiaodong Zou[2] and Mike S. Dadachov

Structural Chemistry, Stockholm University, S-106 91 Stockholm, Sweden

Received May 22, 2000; in revised form August 21, 2000; accepted September 15, 2000; published online December 21, 2000

The hydrothermal reaction in an aqueous mixture of $TiCl_3$, colloidal silica, KF, and KOH yielded colorless prismatic crystals of $K_2TiSi_6O_{15}$. The structure contains one unique TiO_6 octahedron and six unique SiO_4 tetrahedra. The SiO_4 tetrahedra are corner-shared with each other, forming a corrugated $[Si_6O_{15}]_{\infty\infty}$ layer containing four-, six-, and eight-membered rings. These layers are connected by isolated TiO_6 octahedra into a three-dimensional octahedral–tetrahedral mixed anion framework. Four-, five-, and seven-membered rings are formed by mixed SiO_4 tetrahedra and TiO_6 octahedra. The two potassium cations are located in the cage formed by the six- and seven-membered rings. The structure of the title compound is compared with those of related silicates. Crystal data: monoclinic, space group $P2_1$, $a = 6.916(3)$, $b = 12.812(3)$, $c = 7.661(2)$ Å, $\beta = 106.25(4)^\circ$, $V = 651.7(4)$ Å^3, $Z = 2$, and $M = 534.64$. $R_F = 0.0329$ for 2565 unique reflections with $I > 2\sigma(I)$ and 218 parameters.

Key Words: **hydrothermal synthesis; silicates; titanium silicates; framework; mixed framework; crystal structure; X-ray structure determination.**

INTRODUCTION

Natural (minerals) and synthetic mixed framework compounds, with their diverse structures built from common polyhedral units, octahedra and tetrahedra, are of great interest due to their shape-selective catalytic activity and ion-exchange and adsorption properties. Titanium silicates are among those that have been widely studied. For example TS-1 (1) has been widely used as a catalyst for selective oxidation reactions with hydrogen peroxide in industry scale.

There exist more than 70 different titanium silicates. The structures of most of them are mixed anion frameworks (2). During the past decades, great efforts have been made in synthesizing new titanium silicates and their analogs to the minerals. Many synthetic analogues of titanium silicate minerals have been reported, such as natisite $Na_2(TiO)[SiO_4]$ (3, 4) and its polymorph modification $Na_8Ti_{3.5}O_2(OH)_2[SiO_4]_4$ (5), zorite $Na_6[Ti(Ti_{0.9}Nb_{0.1})(Si_6O_{17})_2(O,OH)_5]\cdot 11H_2O$ (6, 7), sitinakite $Na_2(H_2O)_2(Ti_{3.8}Nb_{0.2}(OH)O_5(SiO_4)_2\cdot K(H_2O)_{1.7}$ (8, 9), and fresnoite $Ba_2(TiO)[Si_2O_7]$ (10, 11). Ti analogs of the minerals wadeite $K_2TiSi_3O_9$ (12), nenadkevichite (Na,Ca)(Nb,Ti)$Si_2O_7\cdot 2H_2O$ (13, 14), pharmacosiderite $Me_3HTi_4O_4(SiO_4)_3\cdot 4$–$8H_2O$ (Me = H or alkali metal) (15–18) have also been synthesized. However, only a few novel titanium silicates, such as ETS-10 (19–21) and JDF-L1 (22) have been prepared. Both hydrothermal crystallization and high temperature solid state ceramic methods have been used for synthesis of titanium silicates. Many titanium silicates have open mixed-framework structures and show great potential as ion-exchange compounds (7–9, 14–21, 23).

Recently we have synthesized several new mixed framework titanium silicates, a rhombohedrally distorted $Na_4[Ti_4O_4(SiO_4)_3]\cdot 6H_2O$ (24), an orthorhombic $K_2TiSi_3O_9\cdot H_2O$ (25), and $Na_3(Na,H)Ti_2O_2[Si_2O_6]\cdot 2.2H_2O$ (26), and determined their crystal structures. As a part of our ongoing search for new mixed framework titanium silicates, we report here the synthesis and crystal structure of a novel tetrahedral–octahedral mixed framework of anhydrous potassium titanium silicate $K_2TiSi_6O_{15}$.

EXPERIMENTAL

Synthesis

The title compound $K_2TiSi_6O_{15}$ was synthesized under hydrothermal conditions from aqueous alkaline potassium titanium silicate mixture, containing titanium(III) chloride,

[1] See NAPS Document No. 00000 for 00 pages of supplementary material. This is not a multiarticle document. Order from NAPS c/o Microfiche Publications, P. O. Box 3513, Grand Central Station, New York, NY 10163-3513. Remit in advance in U.S. funds only $7.75 for photocopies or $5.00 for microfiche. There is a $25.00 invoicing charge on all orders filled before payment. Outside the United States and Canada, add postage of $4.50 for the first 20 pages and $1.00 for each 10 pages of material thereafter, or $5.00 for the first microfiche and $1.00 for each microfiche thereafter.

[2] To whom correspondence should be addressed. Fax: + 46 8 16 31 18. E-mail: zou@struc.su.se.

0022-4596/01 $35.00

colloidal silica Ludox HS-40, potassium fluoride and potassium hydroxide. KOH (10.240 g) and 2.531 g Ludox (HS-40, Aldrich) were added to 59.974 g distilled water. KF (0.968 g) and then 5.760 g $TiCl_3$ solution (15wt% $TiCl_3$, 10wt% HCl, Aldrich) were added under continuous stirring. Finally 3.084 g KOH was added to increase the pH to 13.0. The final molar ratio is 1.0 $TiCl_3$:3.0 SiO_2:3.0 KF:42 KOH: $\sim$600 H_2O. About 10 ml of this mixture was sealed in a 23-ml Teflon-lined autoclave (Parr, USA) and heated at 488 K under autogeneous pressure for 212 h. The products contained three crystalline phases with different morphologies: large spherical particles ($\sim$120 μm) formed by prismatic crystal rods (Fig. 1a, phase A) dominated, small spherical particles ($\sim$50 μm) of aggregated crystal plates (Fig. 1b, phase B), and thin plates ($\sim$2 μm wide) (Fig. 1c, phase C). The large spherical particles, which were about $\frac{2}{3}$ of the total products, were separated from the other phases by washing and decanting the mixture with distilled water. They were then filtered and dried at 328 K. The formation of the large spherical particles of the title compound $K_2TiSi_6O_{15}$, occurred only within a narrow range of pH (13.0 $\pm$ 0.5) and molar ratio of Ti:Si (1:3). When the time for the synthesis was reduced to 100 h, only the thin plates (phase C) and some amorphous material were obtained.

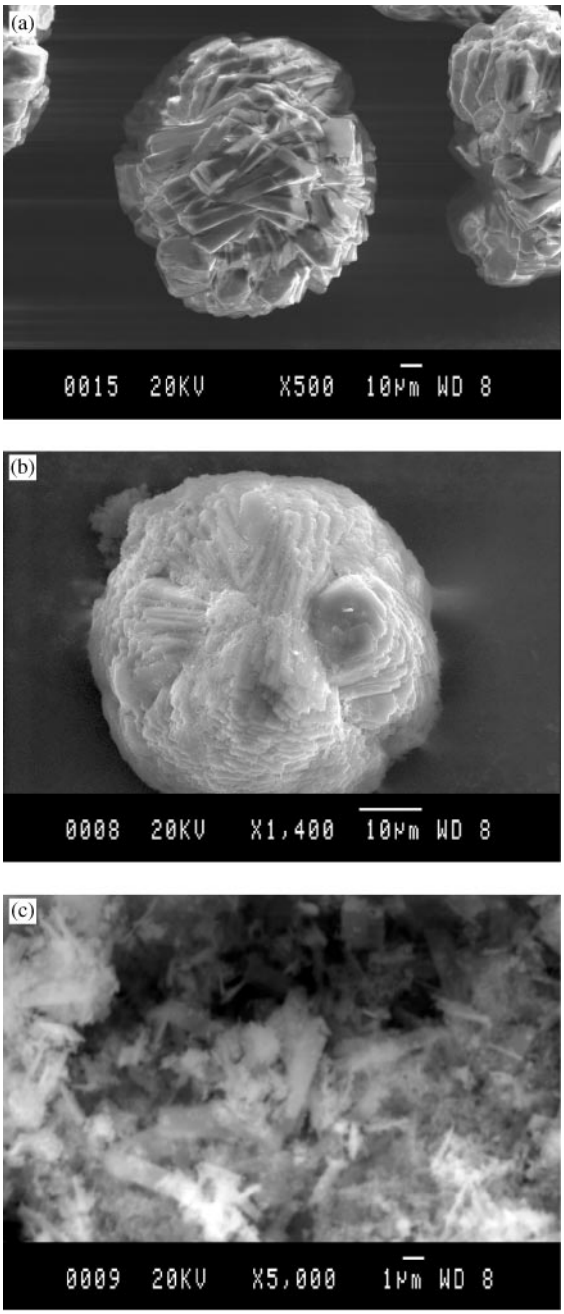

FIG. 1. Scanning electron micrographs of the different phases found in the synthesis. (a) Phase A (the title compound $K_2TiSi_6O_{15}$), (b) phase B ($K_2TiSi_3O_9 \cdot H_2O$), and (c) phase C (new, with a composition of $K_2Ti_4Si_4O_{17} \cdot nH_2O$) and some remaining amorphous material.

Analytical Methods

X-ray powder diffraction analysis was performed on a Guinier–Hägg focusing camera, with Cu$K\alpha_1$ radiation. Fine silicon powder was used as an internal standard. The X-ray powder diffraction patterns indicated that phases A and C were new, while phase B was $K_2TiSi_3O_9 \cdot H_2O$ (25). In order to test the thermal stability of the phase C, X-ray powder diffraction patterns of the phase C were also collected at different temperatures from the room temperature up to 900°C in air on a Huber Imaging Plate Guinier Camera 670 with a heating facility.

Quantitative energy dispersive spectroscopy (EDS) analysis was performed on a JEOL JSM820 scanning electron microscope equipped with a LINK AN1000 system which gave the compositions K:Ti:Si = 1.8:1.0:6.0 for phase A and K:Ti:Si = 1:2:2 for phase C.

Structure Solution and Refinement

Among the three crystalline phases, only phase A was suitable for single crystal X-ray diffraction. A transparent, twin-like prismatic crystal of phase A with dimensions $0.020 \times 0.025 \times 0.10$ mm was selected for single crystal X-ray diffraction analysis. Intensity data were collected at 293 K on a STOE IPDS diffractometer using graphite-monochromatized Mo$K\alpha$ radiation (0.71073 Å) from a rotating anode generator. The distance between the crystal and the detector was 60 mm so that diffraction data between 10.72 and 0.75 Å ($2\theta = 3.8$–$56.3°$) could be collected. Two hundred exposures (ϕ between 0 and 200°) were recorded with a ϕ increment of 1.0°.

The unit cell of phase A, the title compound, was found to be monoclinic with lattice parameters $a = 6.916(3)$, $b = 12.812(3)$, $c = 7.661(2)$ Å, $\beta = 106.25(4)°$ and a cell volume of 651.7(4) $Å^3$, refined using 1003 reflections. No indication of

twinning was found from reciprocal space. A total of 5198 reflections were integrated with a dynamic profile function using effective mosaic spread of 0.010.

Two space groups, $P2_1$ and $P2_1/m$, were consistent with the systematic extinctions. Analysis of the statistical distribution of the normalized structure factors, i.e., $|\langle E^2 - 1\rangle|$, indicated that the structure was acentric and the space group was $P2_1$. This was also confirmed later by the successful solution and refinement of the structure.

The crystal structure of the title compound was solved by direct methods, using the SHELXS-97 (27) software package. The composition was $K_2TiSi_6O_{15}$, which agreed with that obtained by EDS analysis. The nine unique nonoxygen atoms were found directly by direct methods and all the 15 unique oxygen atoms could be located easily from the difference Fourier map. Structure refinement was carried out by SHELXL-97 (28) using atomic scattering factors for neutral atoms. The Flack parameter x (29), estimated by SHELXL-97, was 0.46(7), indicating that the crystal was an inversion twin. Due to the twinning, it was difficult to estimate the shape using X-SHAPE (30) and very little improvement was obtained by numerical absorption correction using X-RED (31). An empirical absorption correction was applied using DIFABS (32), prior to the refinement of anisotropic thermal displacement parameters. The structure was finally refined anisotropically against the intensities, resulting in a final $R1$ index of 3.29% and a weighted Rw index of 7.36% for 2565 reflections with $I > 2\sigma(I)$. The crystallographic data and the results of the structure refinement are given in Table 1.

TABLE 1
Crystal Data and Structure Refinement for $K_2TiSi_6O_{15}$

Crystal data	
Empirical formula	K2 O15 Si6 Ti
Structural formula	$K_2[(TiO_3)(SiO_2)_6]$
Formula weight	534.64
Space group	$P2_1$ (No. 4)
a, b, c [Å]	6.916(3) 12.812(3) 7.661(2)
α, β, γ [°]	90 106.25(4) 90
Z, Volume [Å^3]	2, 651.7(4)
D(calc) [g/cm^3]	2.724
F(000)	528
μ (MoKa) [mm^{-1}]	1.936
Data collection	
Radiation [Å]	Mo$K\alpha$, 0.71073
Theta min-max [°]	3.1, 27.9
Scan(type and range) [°]	Stoe IPDS diffractometer, area detector scans
Data set	$-7 <= h <= 7$, $-14 <= k <= 14$, $-8 <= l <= 8$
No. measured, unique refls., R(int)	5198, 2921, 0.049
No. unique refls. with $I > 2\sigma(I)$	2565
Absorption correction	Empirical (DIFABS, Walker and Stuart, 1983)
T_{min}, T_{max}	0.556, 0.867
Refinement	
Refinement method	Full-matrix least-squares on F^2
No. unique refls., No. parameters	2921, 218
Final R indices ($I > 2\sigma(I)$) $R1$, w$R2$, S	0.0329, 0.0736, 0.980
Final R indices (all data) $R1$, w$R2$,	0.0415, 0.0765
$w = 1/[\sigma^2(F_o^2) + (0.0432P)^2]$ where	$P = (F_o^2) + 2F_c^2)/3$
Max. and min. residual dens. [e/Å^3]	0.455, −0.471

RESULTS AND DISCUSSION

Structure Description

Atomic coordinates and isotropic displacement parameters of the title compound are given in Table 2 and selected bond distances and angles in Table 3. The results of a bond-valence calculation, according to the method of Pyatenko (33), are shown in Table 4.

Structure topology. There are 24 crystallographically unique atoms, 2 potassium, 1 titanium, 6 silicon, and 15 oxygen. An ORTEP presentation of the asymmetric unit, with all the atoms labeled, is shown in Fig. 2. The polyhedral presentations of the structure model are shown in Fig. 3a (along the c axis) and Fig. 3b (along the a axis). The principal structure motif in $K_2TiSi_6O_{15}$ can be described as corrugated $[Si_6O_{15}]_{\infty\infty}$ layers. The layers are parallel to the ab plane, zigzagged along the b axis. The building units of the $[Si_6O_{15}]_{\infty\infty}$ layers are four- and six-membered rings, which are connected to each other forming chair-like eight-membered rings (Fig. 3a). The $[Si_6O_{15}]_{\infty\infty}$ layers are connected by isolated TiO_6 octahedra and stacked along the c axis to form a three-dimensional mixed framework (Fig. 3b). Three types of mixed rings are formed: 4-(T–T–T–O_h), 5-(T–T–T–T–O_h) and 7-(T–T–O_h–T–T–T–T–O_h) membered rings ($T = SiO_4$ tetrahedron and $O_h = TiO_6$ octahedron). The two potassium cations are located in the cage formed by the six- and seven-membered rings.

TiO_6 octahedra. The only crystallographically unique TiO_6 octahedron is slightly distorted (Table 3), with cation-anion distances (Ti–O) between 1.910 and 1.992 Å (average 1.953 Å) and O–Ti–O angles between 84.81 and 93.42°. This is characteristic for Ti octahedra observed in silicate structures with isolated TiO_6 units.

SiO_4 tetrahedra. All the six SiO_4 tetrahedra are corner-shared either with each other or with TiO_6 octahedra. The Si–O bond lengths are in the range of 1.576–1.647 Å, similar to those found in other silicates including anhydrous titanium/zirconium silicates. The Si–O distances of all oxygen atoms involved in the Ti–O–Si bridging are systematically shorter (1.576–1.594 Å) than those in the Si–O–Si bridging (1.615–1.647 Å). The Si–O bonds are slightly oversaturated for those oxygen atoms involved in Ti–O–Si bridging (average bond valence 1.15) compared with those involved only in Si–O–Si bridging (average bond valence 0.97).

TABLE 2
Fractional Atomic Coordinates and Equivalent Isotropic Displacement Parameters (Å^2) for $K_2TiSi_6O_{15}$

Atom	x	y	z	U(eq)
Ti1	0.7564(1)	0.2495(1)	0.2487(1)	0.0082(2)
Si1	0.0069(2)	0.6780(1)	0.3311(2)	0.0089(2)
Si2	0.4502(2)	0.6661(1)	0.4433(2)	0.0085(2)
Si3	0.6714(2)	0.5090(1)	0.2924(2)	0.0085(2)
Si4	0.0127(2)	0.8423(1)	0.0441(2)	0.0089(2)
Si5	0.5439(2)	0.3340(1)	− 0.1641(2)	0.0090(2)
Si6	0.3061(2)	0.5069(1)	− 0.0688(2)	0.0082(2)
K1	0.1943(2)	0.4064(1)	0.4206(2)	0.0296(3)
K2	0.2022(2)	0.1081(1)	0.1500(2)	0.0267(3)
O1	0.2352(5)	0.8825(3)	0.1629(5)	0.0141(7)
O2	0.5375(5)	0.7588(3)	0.3409(5)	0.0131(6)
O3	0.7333(5)	0.3911(3)	0.3346(5)	0.0150(7)
O4	0.2064(5)	0.6088(3)	− 0.1702(5)	0.0133(6)
O5	0.5585(5)	0.2779(3)	0.0241(5)	0.0127(7)
O6	0.0235(5)	0.7927(3)	− 0.1431(5)	0.0125(7)
O7	− 0.1330(5)	0.5755(3)	0.2778(5)	0.0160(7)
O8	0.5889(5)	0.5620(3)	0.4533(5)	0.0129(7)
O9	− 0.1358(5)	0.9435(2)	0.0014(5)	0.0126(6)
O10	0.4997(5)	0.5284(3)	0.1028(5)	0.0165(7)
O11	− 0.0757(5)	0.7604(3)	0.1649(5)	0.0142(6)
O12	0.3861(5)	0.4318(3)	− 0.2082(5)	0.0122(6)
O13	0.2265(5)	0.6356(3)	0.3191(5)	0.0149(7)
O14	0.4519(5)	0.7006(3)	0.6437(5)	0.0123(6)
O15	0.0245(5)	0.7260(3)	0.5265(5)	0.0132(7)

Note. U(eq) is defined as one third of the trace of the orthogonalized U_{ij} tensor.

Cation environment around K ions. The framework has large voids in which the K^+ ions are trapped as charge-compensating countercations. Both potassium cations are nine-coordinated and exhibit similar framework–oxygen environments (Figs. 4a and 4b), with four short, three intermediate and two long K–O distances. The K1–O

TABLE 3
Selected Bond Distances (Å) and Bond Angles (°) for $K_2TiSi_6O_{15}$

TiO_6 octahedron			
Ti1–O3	1.952(3)	O3–Ti1–O15_e	87.87(15)
Ti1–O4_a	1.940(3)	O3–Ti1–O14_g	90.90(14)
Ti1–O15_e	1.972(4)	O3–Ti1–O5_h	91.17(16)
Ti1–O14_g	1.952(3)	O3–Ti1–O6_h	91.28(14)
Ti1–O5_h	1.910(4)	O4_a–Ti1–O15_e	89.61(15)
Ti1–O6_h	1.992(3)	O4_a–Ti1–O14_g	90.61(14)
⟨Ti–O⟩	1.953	O4_a–Ti1–O5_h	91.25(15)
		O4_a–Ti1–O6_h	87.12(14)
		O14_g–Ti1–O15_e	93.42(14)
		O6_h–Ti1–O15_e	84.81(14)
		O5_h–Ti1–O14_g	90.80(14)
		O5_h–Ti1–O6_h	91.00(14)
		⟨O–Ti–O⟩	90.0

TABLE 3—*Continued*

$Si1O_4$ tetrahedron		$Si4O_4$ tetrahedron	
Si1–O7	1.615(4)	Si4–O1	1.637(4)
Si1–O11	1.630(3)	Si4–O6	1.589(4)
Si1–O13	1.639(3)	Si4–O9	1.630(3)
Si1–O15	1.591(4)	Si4–O11_c	1.626(3)
⟨Si1–O⟩	1.619	⟨Si4–O⟩	1.620
O7–Si1–O11	106.0(2)	O1–Si4–O6	110.7(2)
O7–Si1–O13	102.4(2)	O1–Si4–O9	107.6(2)
O7–Si1–O15	115.8(2)	O1–Si4–O11_c	109.4(2)
O11–Si1–O13	107.4(2)	O6–Si4–O9	108.8(2)
O11–Si1–O15	113.7(2)	O6–Si4–O11_c	112.1(2)
O13–Si1–O15	110.6(2)	O9–Si4–O11_c	108.1(2)
⟨O–Si1–O⟩	109.4	⟨O–Si4–O⟩	109.4
$Si2O_4$ tetrahedron		$Si5O_4$ tetrahedron	
Si2–O2	1.631(3)	Si5–O1	1.647(3)
Si2–O8	1.632(3)	Si5–O2	1.628(4)
Si2–O14	1.594(3)	Si5–O5	1.588(3)
Si2–O13_c	1.621(4)	Si5–O12	1.634(3)
⟨Si2–O⟩	1.620	⟨Si5–O⟩	1.624
O2–Si2–O8	109.0(2)	O1–Si5–O2	109.4(2)
O2–Si2–O14	110.9(2)	O1–Si5–O5	110.0(2)
O2–Si2–O13_c	108.3(2)	O1–Si5–O12	106.0(2)
O8–Si2–O14	109.6(2)	O2–Si5–O5	114.0(2)
O8–Si2–O13_c	106.5(2)	O2–Si5–O12	103.0(2)
O14–Si2–O13_c	112.3(2)	O5–Si5–O12	113.8(2)
⟨O–Si2–O⟩	109.4	⟨O–Si5–O⟩	109.4
$Si3O_4$ tetrahedron		$Si6O_4$ tetrahedron	
Si3–O3	1.579(3)	Si6–O4	1.576(3)
Si3–O7	1.629(3)	Si6–O9	1.629(3)
Si3–O8	1.643(3)	Si6–O12_c	1.644(3)
Si3–O10	1.618(4)	Si6–O10_l	1.616(4)
⟨Si3–O⟩	1.617	⟨Si6–O⟩	1.616
O3–Si3–O7	109.4(2)	O4–Si6–O9	108.3(2)
O3–Si3–O8	111.9(2)	O4–Si6–O12_c	110.2(2)
O3–Si3–O10	114.8(2)	O4–Si6–O10_l	114.1(2)
O7–Si3–O8	107.8(2)	O9–Si6–O12_c	108.6(2)
O7–Si3–O10	105.9(2)	O9–Si6–O10_l	109.6(2)
O8–Si3–O10	106.8(2)	O10_l–Si6–O12_c	106.0(2)
⟨O–Si3–O⟩	109.4	⟨O–Si6–O⟩	109.4
K1 polyhedron		K2 polyhedron	
K1–O6_m	2.668(4)	K2–O14	2.741(4)
K1–O12	2.800(4)	K2–O6_m	2.826(4)
K1–O15	2.853(3)	K2–O4_g	2.873(3)
K1–O2	2.908(4)	K2 –O1_g	2.898(4)
K1–O13_f	3.062(4)	K2–O11_n	3.035(4)
K1–O3_f	3.076(4)	K2–O8	3.036(4)
K1–O7_f	3.102(4)	K2–O9_g	3.117(4)
K1–O9_m	3.180(4)	K2–O7_n	3.204(4)
K1–O8_i	3.332(4)	K2–O10_n	3.359(4)

Note. Translation of symmetry code to equivalent positions: a = $-1+x, -1+y, z$; b = $-1+x, y, z$; c = $1+x, y, z$; d = $1+x, 1+y, z$; e = $-x, -\frac{1}{2}+y, 1-z$; f = $-x, \frac{1}{2}+y, 1-z$; g = $1-x, -\frac{1}{2}+y, 1-z$; h = $1-x, -\frac{1}{2}+y, 2-z$; i = $1-x, \frac{1}{2}+y, 1-z$; j = $1-x, \frac{1}{2}+y, 2-z$; k = $2-x, -\frac{1}{2}+y, 2-z$; l = $2-x, \frac{1}{2}+y, 2-z$; m = $-x, -\frac{1}{2}+y, 1-z$; n = $-x, -\frac{1}{2}+y, 1-z$; o = $1-x, -\frac{1}{2}+y, 1-z$;

TABLE 4
Bond-Valence Sum in the Structure of $K_2TiSi_6O_{15}$

	Ti	Si1	Si2	Si3	Si4	Si5	Si6	K1	K2	$\sum V_{ij}$	$\lvert\Delta_i\rvert$
O1					0.937	0.911			0.120	1.968	0.032
O2			0.962			0.984		0.118		2.064	0.064
O3	0.667			1.150				0.102		1.919	0.081
O4	0.690						1.159		0.123	1.972	0.028
O5	0.742					1.147				1.889	0.111
O6	0.603				1.124			0.146	0.128	2.001	0.001
O7		1.008		0.950				0.100	0.094	2.152	0.152
O8			0.951	0.909				0.084	0.107	2.051	0.051
O9					0.964		0.947	0.094	0.100	2.105	0.105
O10				0.990			0.994		0.083	2.067	0.067
O11		0.961			0.975				0.107	2.043	0.043
O12						0.959	0.900	0.130		1.989	0.011
O13		0.919	0.983					0.104		2.006	0.006
O14	0.667		1.104						0.138	1.909	0.091
O15	0.631	1.111						0.123		1.865	0.135
SUM	4.00	4.00	4.00	4.00	4.00	4.00	4.00	1.00	1.00	30.0	6.5%

distances are between 2.668–2.908 Å, 3.062–3.102 Å, and 3.180–3.332 Å and the K2–O distances between 2.741–2.898 Å, 3.035–3.117 Å, and 3.204–3.359 Å, respectively. The thermal displacement parameters of both potassium atoms are larger than those of the framework atoms (Table 2), similar to what has been found in other titanium silicate framework structures.

Crystal Chemical Relations

The new compound $K_2TiSi_6O_{15}$ has several structural similarities with other silicates, although it is not isostructural with any of them. It has the same/similar formula as many silicate minerals and synthetic silicates, for example the isostructural pair davanite $K_2TiSi_6O_{15}$ (34) and dalyite $K_2ZrSi_6O_{15}$ (35), the synthetic epididymite $K_2Be_2Si_6O_{15}$ (36), hydrated armstrongite $CaZrSi_6O_{15}\cdot 2.5H_2O$ (37), $Cs_2TiSi_6O_{15}$ (38), $Cs_2ZrSi_6O_{15}$ (39), elpidite $Na_2ZrSi_6O_{15}\cdot 3H_2O$ (40), $K_2CeSi_6O_{15}$ (41), $K_2GeSi_6O_{15}$ (42), and

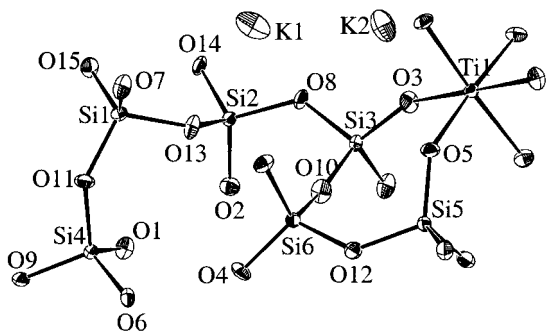

FIG. 2. An ORTEP plot of the asymmetric unit of $K_2TiSi_6O_{15}$ showing the atomic labeling scheme.

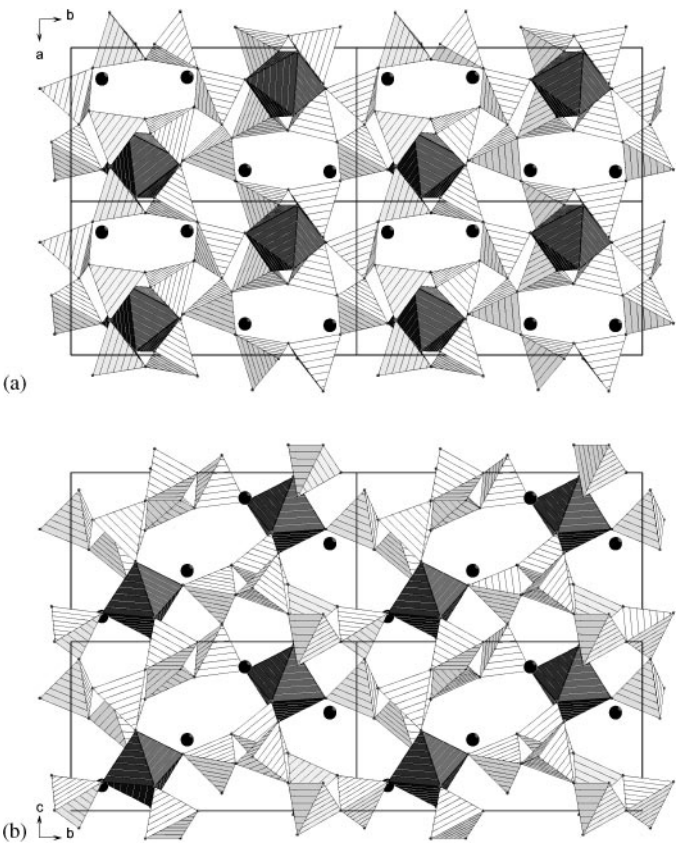

FIG. 3. The structure of the title compound $K_2TiSi_6O_{15}$, (a) viewed along the *c* axis showing the $[Si_6O_{15}]_{\infty\infty}$ layer with four-, six-, and eight-membered rings constructed from tetrahedral units. The isolated TiO_6 octahedra are located in the middle of the four-rings in this projection, (b) viewed along the *a* axis showing a side view of the $[Si_6O_{15}]_{\infty\infty}$ layer and the connection of the layers by isolated TiO_6 octahedra. The TiO_6 octahedra are in dark gray, SiO_4 tetrahedra light gray, and potassium ions in filled black circles.

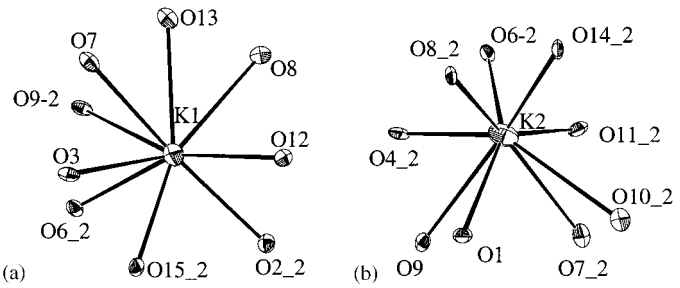

FIG. 4. ORTEP drawings of the environments for potassium ions in $K_2TiSi_6O_{15}$. (a) Around K1 and (b) around K2.

sazhinite $Na_2CeSi_6O_{14}(OH)\cdot 1.5(H_2O)$ (43). All these structures have infinite corrugated $[Si_6O_{15}]_{\infty\infty}$ layers. Three of them, namely davanite, epididymite and armstrongite are more closely related to the title compound.

The Si–Si connections in the $[Si_6O_{15}]_{\infty\infty}$ layers, for the title compound (Fig. 5a), davanite (Fig. 5b), armstrongite (Fig. 5c), and epididymite (Fig. 5d) constitute an interesting sequence of structures. The building units of the $[Si_6O_{15}]_{\infty\infty}$ layers are the same in all the structures, i.e., four-, six-, and eight-membered SiO_4 tetrahedral rings. The eight-membered rings form a chair-like unit (highlighted in Fig. 5). In one direction (perpendicularly in Fig. 5), the chair-like units are connected by two shared SiO_4 tetrahedra-forming silicon–oxygen ribbons, similar to the eight-membered rings in the mineral xonotlite $Ca_6(Si_6O_{17})(OH)_2$ (44). In the other direction (horizontally in Fig. 5), the chair-like units are connected by two corner-sharing SiO_4 tetrahedra. As a result, four- and six-membered rings are formed in all the cases. The relative orientation of the chair-like units in each structure is different. In davanite (Fig. 5b) and armstrongite, all the chair-like units are oriented in the same way (Fig. 5c), while in the title compound (Fig. 5a) and epididymite (Fig. 5d) they are oriented differently, such that a twofold screw axis is generated (horizontally in Fig. 5).

The $[Si_6O_{15}]_{\infty\infty}$ layers are complex and very much corrugated, as seen from the side view of the $[Si_6O_{15}]_{\infty\infty}$ layers in Fig. 6. Among these four silicates, the wave amplitudes for the $[Si_6O_{15}]_{\infty\infty}$ layers of the title compound and epididymite are much larger than those for the $[Si_6O_{15}]_{\infty\infty}$ layers of davanite and armstrongite.

The $[Si_6O_{15}]_{\infty\infty}$ layers of the silicates discussed above are connected into three-dimensional mixed frameworks by octahedrally coordinated atoms (Ti and Zr) (Fig. 7), except for epididymite where the layers are connected by pairs of beryllium–oxygen tetrahedra. The octahedra in the title compound are zigzagged while those in davanite (Fig. 7b) and armstrongite (Fig. 7c) are lying on a straight line. There are only two types of titanium involved polyhedral ring systems in the structures of davanite and armstrongite:

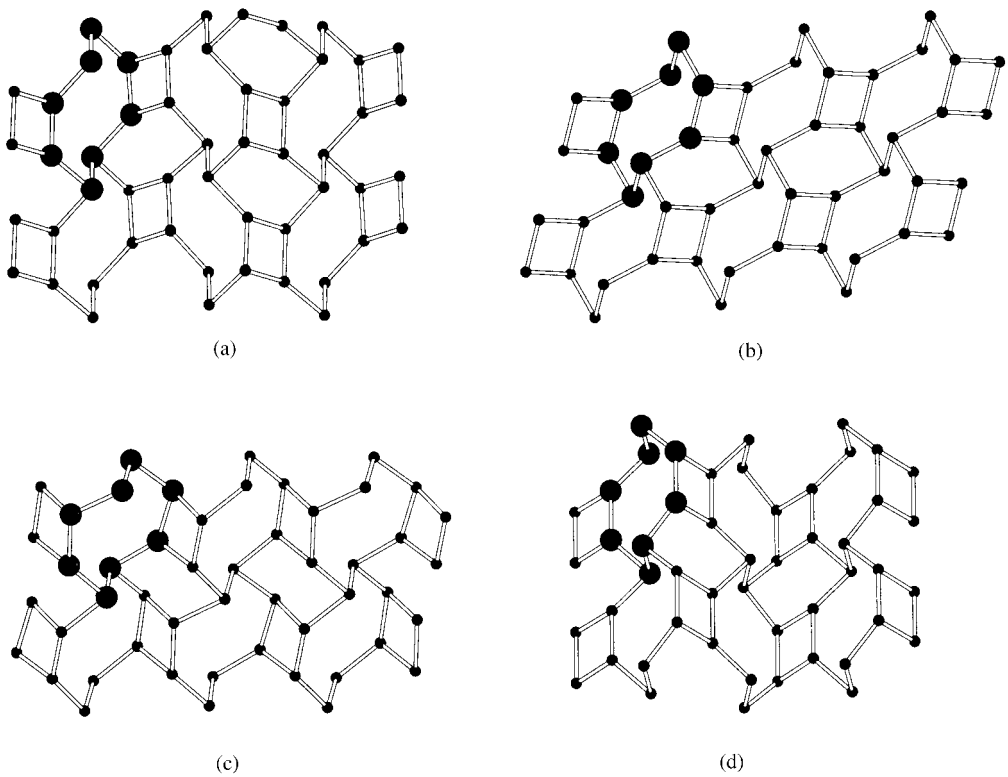

FIG. 5. Comparison of the $[Si_6O_{15}]_{\infty\infty}$ layers in different compounds. All the layers have four, six-, and chair-like eight-membered rings. The latter is highlighted in each structure. (a) The title compound $K_2TiSi_6O_{15}$, (b) davanite $K_2TiSi_6O_{15}$, (c) armstrongite $CaZrSi_6O_{15}\cdot 2.5H_2O$, and (d) epididymite $K_2Be_2Si_6O_{15}$. Only the Si–(O)–Si connections are drawn for clarity.

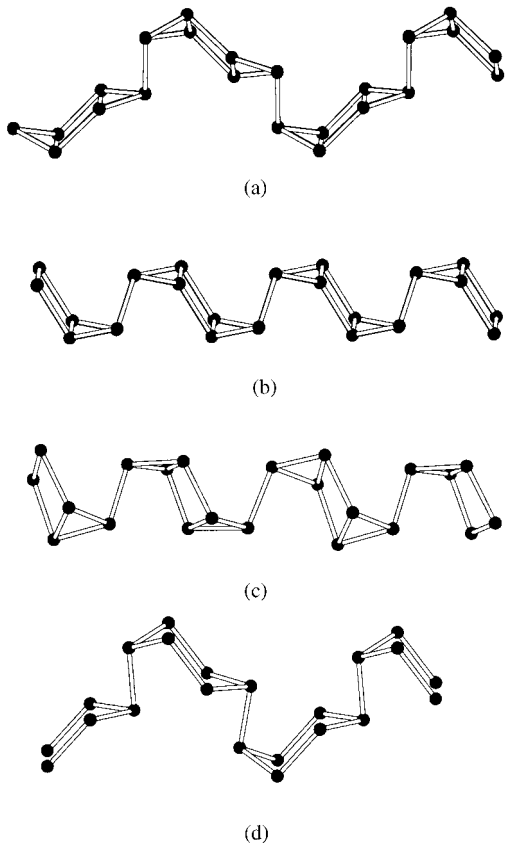

FIG. 6. The $[Si_6O_{15}]_{\infty\infty}$ layers viewed perpendicular to the layers. (a) The title compound $K_2TiSi_6O_{15}$, (b) davanite $K_2TiSi_6O_{15}$, (c) armstrongite $CaZrSi_6O_{15} \cdot 2.5H_2O$, and (d) epididymite $K_2Be_2Si_6O_{15}$. Only the Si–(O)–Si connections are drawn.

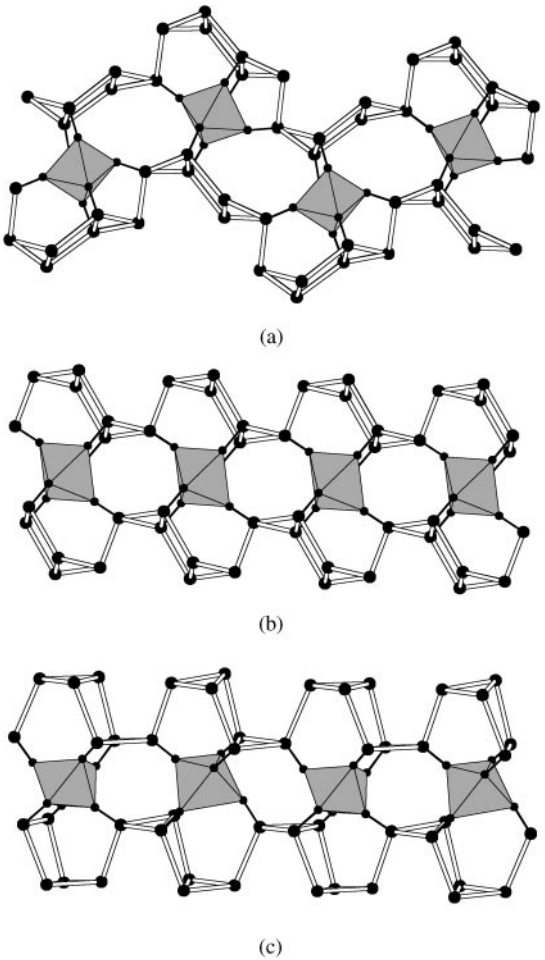

FIG. 7. Comparison of the connection of the $[Si_6O_{15}]_{\infty\infty}$ layers by isolated octahedra. (a) The tile compound $K_2TiSi_6O_{15}$, (b) davanite $K_2TiSi_6O_{15}$, and (c) armstrongite $CaZrSi_6O_{15} \cdot 2.5H_2O$. Only the Si–(O)–Si connections are drawn.

5-(T–T–T–T–O_h) and 6-(T–T–O_h–T–T–O_h) rings, which are different from those in the title compound (4-(T–T–T–O_h), 5-(T–T–T–T–O_h), and 7-(T–T–O_h–T–T–T–T–O_h) rings).

In addition to the layered configuration $[Si_6O_{15}]_{\infty\infty}$, structures of Si_6O_{15}-based silicates can also adapt double-chain, double ring, and framework configurations, as reviewed by Haile and Wuensch (45).

Thermal Behavior

X-ray powder diffraction showed that the title compound, $K_2TiSi_6O_{15}$, was stable up to 750°C in air and then decomposed into cristobalite SiO_2, Si, and anatase TiO_2.

CONCLUSIONS

The geometry and orientation of the building units and the way they are connected can result in a great variation of the final crystal structures. Even for compounds with the same stoichiometry, as for example here davanite and the title compound, the structure can be different. This is a good illustration of the fact that crystallization conditions, for example temperature and initial composition, are the main factors that determine the structure of a polymorph.

The discovery of the new $K_2TiSi_6O_{15}$ makes an important contribution to hydrothermal methods and crystal chemistry of titanium silicates as well as mixed anion framework compounds in general.

ACKNOWLEDGMENT

Ken Okamoto was involved in the early experiments of titanium silicate syntheses. This work is supported by the Swedish Natural Science Research Council (NFR).

REFERENCES

1. B. Notari, *Catal. Today* **18,** 163 (1993).
2. Yu. A. Pyatenko, A. A. Voronkov, and Z. V. Pudovkina, "The Mineralogical Crystal Chemistry of Titanium". Nauka, Moscow, 1976. [in Russia]

3. A. B. Nikitin, B. B. Ilyukhin, B. N. Litvin, O. K. Melnikov, and N. V. Belov, *Kristallografiya* **157,** 1355 (1964).
4. Yu. Menshikov, *Zap. Vses. Mineral. Ova.* **104,** 314 (1976).
5. E. B. Sokolova, A. N. Yamnova, Yu. K. Egorov-Tismenko, and A. P. Chomyakov, *Dokl. Akad. Nauk SSSR* **284,** 1136 (1985).
6. A. N. Mer'kov, I. V. Bussen, E. A. Goiko, E. A. Kul'chitskaya, Y. P. Men'shikov, and A. P. Nedorezova, *Zap. Vses. Mineral. Ova.* **102,** 54 (1973).
7. P. A. Sandomirskii and N. V. Belov, *Kristallografiya* **24,** 1198 (1979).
8. E. B. Sokolova, R. K. Rastsvetaeva, V. Andrianov, Yu. K. I'Egorov-Tismenko, and Yu. P. Men'shikov, *Dokl. Akad. Nauk SSSR* **307,** 114 (1989).
9. R. G. Anthony, C. V. Philip, and R. G. Dosch, *Waste Manage* **13,** 503 (1993).
10. P. B. Moore and S. J. Louisnathan, *Z. Kristallogr.* **130,** 438 (1969).
11. S. A. Markgraf, A. Halliyal, A. S. Bhalla, R. E. Newnham, and C. T. Prewitt, *Ferroelectrics* **62,** 17 (1985).
12. N. G. Shumyatskaya, V. A. Blinov, A. A. Voronkov, V. V. Ilyukhin, N. V. Belov, and Yu. P. Men'shikov, *Dokl. Akad. Nauk SSSR* **208,** 591 (1973).
13. G. Perrault, C. Boucher, J. Vicat, E. Cannillo, and G. Rossi, *Acta Crystallogr. B* **29,** 1432 (1973).
14. J. Rocha, P. Brandao, Z. Lin, A. Kharlamov, and M. W. Anderson, *Chem. Commun.* **5,** 669 (1996).
15. D. M. Chapman and A. L. Roe, *Zeolites* **10,** 730 (1990).
16. W. T. A. Harrison, T. E. Gier, and G. D. Stucky, *Zeolites* **15,** 408 (1995).
17. E. A. Behrens and A. Clearfield, *Microporous Mater.* **11,** 65 (1997).
18. A. I. Bortun, L. N. Bortun, D. M. Poojary, O. Xiang, and A. Clearfield, *Chem. Mater.* **12,** 294 (2000).
19. S. M. Kuznicki, U.S. patent 4853202, 1989.
20. M. W. Anderson, O. Terasaki, T. Ohsuna, A. Phillppou, S. P. Mackay, A. Ferrrira, J. Rocha, and S. Lidin, *Nature* **367,** 347 (1995).
21. X. Wang and A. J. Jacobson, *Chem. Commun.* **11,** 973 (1999).
22. M. A. Roberts, G. Sankar, J. M. Thomas, R. H. Jones, H. Du, J. Chen, W. Pang, and R. Xu, *Nature* **381,** 401 (1996).
23. D. M. Poojary, A. I. Bortun, L. N. Bortun, and A. Clearfield, *Inorg. Chem.* **36,** 3072 (1997).
24. M. S. Dadachov and W. T. A. Harrison, *J. Solid State Chem.* **134,** 409 (1997).
25. M. S. Dadachov and A. Le Bail, *Eur. J. Solid State Inorg. Chem.* **34,** 381 (1997).
26. M. S. Dadachov, J. Rocha, A. Ferreira, Z. Lin, and M. W. Anderson, *Chem. Commun.* **24,** 2371 (1997).
27. G. M. Sheldrick, "SHELXS97—Program for the Solution of Crystal Structures." Univ. of Göttingen, Germany, 1997.
28. G. M. Sheldrick, "SHELXL97—Programs for Crystal Structure Analysis." Univ. of Göttingen, Germany, 1997.
29. H. D. Flack. *Acta Crystallogr. A* **39,** 876 (1983).
30. STOE & CIE, "X-SHAPE—Crystal Optimization for Numerical Absorption Correction," V1.02/Windows. STOE & CIE, GmbH, Darmstadt, Germany, 1997.
31. STOE & CIE, "XRED—STOE Data Reduction Program," V1.09/Windows. STOE & CIE, GmbH, Darmstadt, Germany, 1997.
32. N. Walker and D. Stuart, *Acta. Crystallogr. A* **39,** 158 (1983).
33. Yu. A. Pyatenko, *Kristallografiya* **17,** 773 (1972).
34. W. Gerbert, O. Medenbach, and O. W. Floerke, *Tschermaks Mineral. Petrogr. Mitt.* **31,** 69 (1983).
35. S. G. Fleet, *Z. Kristallogr.* **121,** 349 (1965).
36. I. S. Naumova, E. A. Pobedimskaya, D. Y. Pushcharovskij, N. V. Belov, and Y. N. Altukhova, *Dokl. Akad. Nauk SSSR* **229,** 856 (1976).
37. A. A. Kashaev and A. N. Sapozhnikov, *Kristallografiya* **23,** 956 (1978).
38. I. E. Grey, R. S. Roth, and M. L. Balmer, *J. Solid State Chem.* **131,** 38 (1997).
39. G. Jolicart, M. Leblanc, B. Morel, Ph. Dehaudt, and S. Dubois, *Eur. J. Solid State Inorg. Chem.* **33,** 647 (1996).
40. E. Cannillo, G. Rossi, and L. Ungaretti, *Am. Mineral.* **58,** 106 (1973).
41. O. G. Karpov, E. A. Pobedimskaya, and N. V. Belov, *Kristallografiya* **22,** 382 (1977).
42. M. G. Mikheeva, N. A. Yamnova, R. K. Rastsvetaeva, D. Yu. Pushcharovskii, and S. L. Sorokina, *Kristallografiya* **37,** 70 (1992).
43. N. G. Shumyatskaya, A. A. Voronkov, and Y. A. Pyatenko, *Kristallografiya* **5,** 728 (1980).
44. K. S. Mamedov and N. V. Belov, *Dokl. Akad. Nauk SSSR* **104,** 615 (1955).
45. S. M. Haile and B. J. Wuensch, *Am. Mineral.* **82,** 1141 (1997).